Supporting Information

Close et al. 10.1073/pnas.1217514110

SI Text 1. Sample Preparation and Analytical Methods

Samples were the same extracts of filters of water-column particulate material described in ref. 1, as obtained from Natural Energy Laboratory of Hawaii Authority (NELHA) seawater pipelines. The total lipid extract (TLE) was subjected to acid hydrolysis in 5% hydrochloric acid in methanol, heated at 70 °C, to convert all free fatty acids and polar lipid fatty acid side chains to fatty acid methyl esters (FAMEs). The same batch of methanol was used for all reactions, and its $\delta^{13}C$ and $\Delta^{14}C$ values were measured separately; these values are used in mass-balance equations that account for the ^{13}C and ^{14}C content of the donor methyl group.

The fraction of TLE containing FAMEs was purified by silica gel chromatography [eluted in 90% (vol/vol) hexane, 10% (vol/vol) ethyl acetate]. Separate aliquots of this fraction were used for three separate gas chromatography (GC) applications: GC-flame ionization detection (FID) to determine relative proportions of individual FAMEs, GC-isotope ratio-monitoring combustion mass spectrometry (GC-C-irMS) to determine $\delta^{13}C$ values of individual FAMEs, and preparative capillary GC (PCGC) to purify and collect individual FAMEs for radiocarbon analysis. GC-mass spectrometry (GC-MS) was also used to identify compounds via their fragmentation patterns. The surface 0.2- to 0.5-μm filter was not measured via GC-MS due to instrument availability and limited sample size; compounds in this sample were identified via comparison of GC-FID retention time with that in other samples.

Separation of FAMEs for radiocarbon analysis by PCGC is described in ref. 2. Briefly, individual FAMEs collected by PCGC were dried under N_2 and flame-sealed on a vacuum line in precombusted quartz tubes with added cupric oxide. Sealed tubes were heated for 5 h at 850 °C to convert purified compounds to CO_2. Individual CO_2 samples were released into a vacuum line, quantified manometrically, cryogenically purified and collected, and flame-sealed into glass tubes. CO_2 samples were sent to accelerator-mass spectrometry (AMS) facilities for conversion to graphite and measurement of natural ^{14}C content (Table S1).

Relative proportions of fatty acids were derived from relative peak area obtained during GC-FID. Absolute sample sizes for radiocarbon analysis (reported in Table S1) were determined via vacuum-line quantification of CO_2.

Prokaryotic cells were counted by fluorescent catalyzed reporter deposition in situ hybridization (CARD-FISH) with probes EUB338 and ARC915, using methods from ref. 3 and the permeabilization method specific for archaeal cells from ref. 4.

Corrections to Radiocarbon Data. Processing blanks and error corrections for our laboratory radiocarbon-preparation procedure were established and reported previously (1, 5). Reported AMS-facility values were corrected for biological fractionation as determined by $\delta^{13}C$ values. Following the error-propagation technique described in ref. 5, these corrected values of $\Delta^{14}C$ and measurement error were corrected for the blanks, uncertainties, and derivatization carbon as described below (Table S1).

Combustion correction. A 1-μg carbon blank can be attributed to the combustion process for purified compounds ($\Delta^{14}C$ value 58.5 ± 208.5‰), and additional error derives from propagation of an ∼1.7% uncertainty in vacuum-line volume and subsequent calculations of sample size. This blank contribution is accounted for in proportion to the size of the sample.

Residual/contaminant correction. $\Delta^{14}C$ values for three of the four sample sets were found to correlate to sample size, indicating an additional source of contamination that contributes a constant mass of carbon to each sample within a given set. Based on a linear projection of the $\Delta^{14}C$ – sample size correlation, a "true" $\Delta^{14}C$ value for a sample of infinite size was derived for each sample set. From this, the size of the contaminant was calculated and included in correction of $\Delta^{14}C$ and corresponding error values, assuming a $\Delta^{14}C$ value of −1,000‰ for the contaminant (i.e., petroleum-derived or otherwise radiocarbon-dead source of carbon). Contaminant sizes for each sample set are detailed in Table S1; size-based correlation is shown in Fig. S1. A "sample set" refers to compounds separated from the same original filter extract and subsequently processed in the same batches through consecutive procedural stages: PCGC, combustion, and vacuum-line quantitation. Values within the sets include replicate measurements from splits of the same CO_2 sample; i.e., the residual must have been introduced downstream of the point of combustion, for example, during graphitization (5). Independent confirmation of a contaminant in the deep sample sets was found by comparing $\delta^{13}C$ values reported from the National Ocean Sciences Accelerator Mass Spectrometry facility against those measured separately by GC-C-irMS. The differences between these two sources of $\delta^{13}C$ measurements for individual compounds correlate well with $\Delta^{14}C$ values ($R^2 = 0.91$), indicating addition of an isotopically constant (and relatively ^{13}C-depleted) end member, possibly in the graphitization process for AMS (Fig. S2).

In the fourth sample set (surface >0.5 μm), $C_{19:0}$ FAME was added as an internal standard previous to PCGC separation. The internal standard was collected by PCGC identically to the other compounds in the sample and analyzed for ^{14}C content. An aliquot of $C_{19:0}$ free fatty acid standard from the original manufacturer's bottle (powder) was also analyzed to determine a true value. The blank- and methyl-corrected $\Delta^{14}C$ value for the PCGC-separated standard was 48‰, whereas the bottled $C_{19:0}$ had a $\Delta^{14}C$ value of 71‰. We assume that the difference can be attributed to an additional carbon blank (again, possibly from the graphitization process) with a $\Delta^{14}C$ value of −1,000‰; by mass balance, we calculate its size to be 1.67 μg of carbon. As above, we corrected the $\Delta^{14}C$ values for other compounds from this batch in proportion to their mass.

Methyl correction. Methanol used in acid hydrolysis/transesterification reactions was previously measured and had a $\delta^{13}C$ value of −39‰ and a $\Delta^{14}C$ value of −1,000‰. Values of $\Delta^{14}C$ for samples were corrected for the addition of one carbon atom (as a methyl group) from this methanol, calculated in proportion to the number of carbon atoms in the fatty acid chain of each individual compound. Compound-specific $\delta^{13}C$ values were similarly corrected for the addition of this methyl group from methanol.

SI Text 2. Authenticity of Environmental Signature (DNA Analysis)

The dissimilarity in bacterial phylogenetic profiles between the surface small sample and the mesopelagic sample led us to conclude that we did not inadvertently incubate an enrichment culture of heterotrophs on the filters during sampling (Fig. S3). The samples were examined by PhyloChip hybridization of DNA amplicons of 16S ribosomal RNA genes. PhyloChip is a microarray chip that is capable of detecting >10,000 operational taxonomic units (OTUs); amplification and hybridization protocols, including signal calibrations against known concentration standards, were performed as defined in refs. 16 and 17). The similarity be-

tween fatty acids in surface and mesopelagic samples is thus an authentic environmental signature and contrasts with the dissimilarity in DNA profiles between the samples.

SI Text 3. Determining the Maximum Sinking Contribution from Fatty Acid Profiles Only

To address the contribution of submicron extra-small particulate organic matter (X-POM) to exported lipids, we model the mesopelagic—or deep (**D**)—lipid and isotopic content as a mixture of surface large POM (**L**, >0.5 μm), surface X-POM (**X**, 0.2–0.5 μm), and in situ mesopelagic biomass (**I**). First, we calculate a boundary on the minimum possible contribution from an in situ population **I**—and thus the maximum contribution from sinking material (**L** + **X**)—using fatty acid profiles only. We construct a mixing model based on the relative abundance of major fatty acids quantifiable in all samples ($C_{14:0}$, $C_{16:1}$, $C_{16:0}$, $C_{18:1}$, and $C_{18:0}$). $C_{17:0}$ was present in all samples but was a minor compound (1–2% of peak area in each sample) and so was not used for the mixing model. We derive the best-fit mixing ratio of surface large (**L**) and small (**X**) fatty acid (FA) profiles to generate a mixture (**M**) that mimics the mesopelagic or deep (**D**) profile. All possible mixing ratios between chromatograms were calculated (0–100% of each end member, stepping by 0.2%). The relative abundance of each compound, i, in mixture **M** was calculated as

$$\chi_{M,i} = f_X \chi_{X,i} + (1 - f_X)\chi_{L,i},$$

where

i = individual fatty acid compound

χ = mass fraction of compound "i" in the measured sample (**X**, small or **L**, large; Table S1) or modeled mixture (**M**). (Mass fraction is defined as the mass of an individual compound—determined by FID peak area relative to a known quantity of a standard—divided by the summed masses of all compounds in the profile that are considered in this model.)

f_X = proportion of total fatty acids from source **X** in the sinking mixture.

We then specify that in total, each deep (**D**) compound i is composed of fractional contributions f_M from a given sinking mixture (**M**) and $1 - f_M$ from the in situ component (**I**):

$$\chi_{D,i} = f_M \chi_{M,i} + (1 - f_M)\chi_{I,i}.$$

To achieve conservation of mass, no solution can be permitted that would allow $(1 - f_M)\chi_{I,i} < 0$ (i.e., negative concentrations are not allowed for any individual in situ component I_*i*). Therefore, the maximum contribution of the calculated mixture **M** is maximized at the highest value of f_M for which $(1 - f_M)\chi_{I,i} \geq 0$ for all compounds *i*. This maximum f_M is found as the minimum among all *i* of $\chi_{D,i}/\chi_{M,i}$, i.e., when for that compound i, $(1 - f_M)\chi_{I,i} = 0$.

We define the best-fit sinking mixture **M** as the combination of the measured distributions **X** and **L** that allows the largest f_M, while still satisfying the conservation of mass requirement above. Of all mixing ratios of **X** and **L**, f_M is maximized at 0.856, corresponding to $f_X = 0.888$ and $f_L = 1 - f_X = 0.112$. This mixture **M** (Fig. S4*B*) generally reproduces the observed compound ratios for the deep sample **D** (Fig. S4*A*), although with some differences. The residuals are calculated by subtracting the best-fit **M** profile from the observed **D** profile, with the concentration of each compound normalized to $C_{16:0}$ [the compound *i* at which $\chi_{D,i}/\chi_{M,i}$ was minimized, i.e., for which $(1 - f_M)\chi_{I,i} = 0$]. These residuals reflect the minimum proportion of the deep profile that must remain unaccounted for by sinking FA. We thus confirm the minimum proportion of these five major fatty acids that must be produced in situ at depth, and we calculate their in situ profile. At minimum, 14.4% of the total peak area of the observed deep profile **D** cannot be accounted for by the best-fit sinking model (i.e., minimum $f_I = 0.144$, maximum $f_M = 0.856$). Under this scenario of minimum in situ production, because f_I is 14.4%, then $f_L \times f_M$ is 9.6% (= 0.112×0.856) and $f_X \times f_M$ is 76% (= 0.888×0.856). As discussed in the main text, the actual contribution f_I can be any value from 14% to 100%; numbers have been rounded to two significant values for the main text

Little is known about the fatty acid production patterns of mesopelagic Bacteria: the distribution of compounds *i* in **I** is instead predicted by subtraction of the modeled mixture **M** from the observed deep profile **D**. In the case of minimal in situ contribution, the proportionally largest in situ signal (largest individual contributor, *i*, to **I**) is contributed by isomers of $C_{18:1}$ (Fig. S4*C*). Examining the mass spectrum for $C_{18:1}$ in all samples reveals that the deep sample contains a large peak in $C_{18:1\omega9}$ isomer that is a minor contributor to both surface samples. This ω9 isomer of $C_{18:1}$ is thus the largest unique contributor to—and thus the likeliest representation of—the in situ mesopelagic contribution.

SI Text 4. Deriving Further Constraints on X + L = M and M + I = D, Using Compound-Specific $\delta^{13}C$ Data

Large variation in measured $\delta^{13}C$ values among individual compounds—both within and between samples—provides an additional means to evaluate permissible mixing ratios. Following refs. 6 and 7, we construct a mass-balance model based on the relative proportion of individual fatty acid compounds within a given sample, along with their $\delta^{13}C$ values. The isotope model is based on the four compounds for which $\delta^{13}C$ values were measurable in all samples: $C_{16:1}$, $C_{16:0}$, $C_{18:1}$, and $C_{18:0}$. We first model the relative fatty acid profile and $\delta^{13}C$ values of hypothetical sinking POM as a mixture (**M**) of the measured small (**X**) and large (**L**) size class, as above. We calculate the projected $\delta^{13}C$ values ($\delta_{M,i}$) across the entire range of possible mixtures (f_X = 0–100% small size class), using data from Table S1, according to

$$\chi_{M,i} = f_X \chi_{X,i} + (1 - f_X)\chi_{L,i}$$

as above, and

$$\delta_{M,i} = \left[f_X \chi_{X,i} \delta_{X,i} + (1 - f_X)\chi_{L,i}\delta_{L,i}\right] / \left[f_X \chi_{X,i} + (1 - f_X)\chi_{L,i}\right],$$

where

i = individual fatty acid compound

χ = mass fraction of fatty acid *i* in the measured sample (**X** or **L**) or modeled mixture (**M**)

f_X = proportion of total fatty acid from source X in modeled sinking mixture (**M**)

$\delta = \delta^{13}C$ value of fatty acid *i* in sample or modeled mixture.

We then consider each iteration of this hypothetical mixed sinking material (**M**) as a contributor to the measured total deep (**D**)

sample. The other end member contributing to the total deep sample is the in situ mesopelagic community (**I**):

$$\chi_{D,i} = f_M \chi_{M,i} + (1 - f_M)\chi_{I,i}; (1 - f_M)\chi_{I,i} \geq 0$$
$$\delta_{D,i} = \left[f_M \chi_{M,i}\delta_{M,i} + (1 - f_M)\chi_{I,i}\delta_{Ii}\right] / \chi_{D,i}.$$

Rearranging, we solve for the proportion and $\delta^{13}C$ value of each fatty acid from the in situ community ($\chi_{\mathbf{I},i}$ and $\delta_{\mathbf{I},i}$, respectively) across the allowable range of **M** and the full range of **X** and **L** (Fig. S5). The range of allowable solutions for each in situ component ($\chi_{\mathbf{I},i}$ $\delta_{\mathbf{I},i}$) is that which achieves isotopic mass balance with the deep sample ($\chi_{\mathbf{D},i}$, $\delta_{\mathbf{D},i}$) within the measurement errors. These ranges are shown outlined in Fig. S5. The conservation of mass condition described above limits the absolute largest contribution of $f_{\mathbf{M}}$ for a given $f_{\mathbf{X}}$ and $f_{\mathbf{L}}$; this limitation is delineated in Fig. S5 by line A, the boundary between shaded areas and white (nonsolution) areas. We thus have calculated $\delta_{\mathbf{I},i}$ for a range of sinking material from 0 to the maximum percentage allowable by profile mixing [satisfying $(1 - f_{\mathbf{M}})\chi_{\mathbf{I},i} \geq 0$] and, within this constraint on $f_{\mathbf{M}}$, for a range of composition in sinking material from 0% to 100% small ($f_{\mathbf{X}}$) surface material. In all cases, we further constrain values of $\delta_{\mathbf{I},i}$ to a maximum value of −16‰ or no more than 2.5‰ more positive than the highest measured value of δ, based on the argument of limited trophic-level enrichment of ^{13}C in bacterial heterotrophy (8, 9); this further limits the allowable results to only those values that fall below line B in Fig. S5 *A* and *B*. Because we thus place a constraint on the maximum allowable $\delta^{13}C$ value for individual in situ compounds, we consider the most conservative (minimum) $\delta^{13}C$ value achieved by calculating over the error ranges for all measured $\delta^{13}C$ values. The maximum contribution from the large size class to the total (i.e., maximum allowable $[f_{\mathbf{M}} \times (1 - f_{\mathbf{X}})]$) is further limited to ≤23% under this constraint (Fig. S5, line B; equivalent to the solution field with dark shading in Fig. 3 of the main text).

Importantly, solving the model in this way does not require that we aim to converge on a single and uniform $\delta^{13}C$ value for the entire in situ mesopelagic community, because isotopic heterogeneity among lipids from living communities is observed elsewhere (e.g., the surface sample here). Instead, the model allows each calculated value of $\delta_{\mathbf{D},i}$ to converge on the measured value of $\delta_{\mathbf{D},i}$ independently; and from the four different compounds modeled (Fig. S5), we derive the boundaries for allowable fractional contributions **X**, **L**, and **I**.

SI Text 5. Predicting the Magnitude of Sinking Bacterial Lipids by Comparison with Sinking Archaeal Lipids

Ingalls et al. (1) calculate that 14 ± 7% of archaeal lipids measured at 670 m are from sinking surface biomass. Average live archaeal cell counts at 500 m depth (the closest measured depth to our sample) in the North Pacific Subtropical Gyre (NPSG) are 2.26×10^4 cells/mL (10) (Table S2). Presuming that all archaeal cells have approximately the same lipid content and that the sinking cells mainly are dead (i.e., their RNA is sufficiently degraded that they would not be counted by the FISH methods of ref. 10), the additional sinking component contributes its lipids without being counted as part of the in situ population. This is consistent with numerous studies that show strain-level heterogeneity in archaeal and bacterial populations as a function of depth in the water column (e.g., ref. 11). If sinking cellular material indiscriminately carried DNA and RNA to depth, it would mask these patterns. Therefore, the in situ population by FISH (2.26×10^4 cells/mL) is equivalent to only 86 ± 7%, or 79–93%, of the total collected archaeal lipids. By this reasoning, the number of "cell equivalents" of total archaeal lipids is 2.43×10^4 to 2.86×10^4 cells/mL, meaning the sinking lipid contribution is equivalent to adding lipids from 1,700–6,000 cells/mL of sinking, surface-derived Archaea to the mesopelagic waters. As explained in the main text, this calculation can be extended to estimate exported bacterial lipids (contributing 31–62% of the total lipids at depth). This estimate does not account for the additional contribution from sinking eukaryotic biomass. As such, it represents a lower bound on the predicted sinking flux, and the total surface contribution must be higher. The lower bound of this range is defined as dashed line D in Fig. S5.

SI Text 6. Predicting the Fraction of Mesopelagic Fatty Acids Derived from in Situ Bacteria, Using ^{14}C Budgets

Total DNA collected from POM at mesopelagic depths should reflect the combined in situ bacterial and archaeal contribution, assuming that eukaryotic cells contribute insignificant DNA at 670 m. Hansman et al. (12) report $\Delta^{14}C$ values for DNA from two size classes of total POM (0.2–0.5 μm and >0.5 μm) (Table S2). Because our sample integrates the total of all POM >0.2 μm, we constrain the mass balance broadly, to cover the entire range of values reported in ref. 12, including error (−157‰ to −69‰). Ingalls et al. (1) measured ^{14}C content in archaeal lipids and by mass-weighted calculation derived an average $\Delta^{14}C$ value of −112‰ for mesopelagic Archaea living in situ. If in situ mesopelagic Archaea and Bacteria are the only two end members contributing to the DNA signature, and mesopelagic bacteria represent 57 ± 12% of the total population at these depths (9), then by isotopic mass balance, the in situ bacterial $\Delta^{14}C$ value could be between −191‰ and −37‰.

Similar to ref. 1, we can then calculate a mass-weighted $\Delta^{14}C$ value for fatty acids measured at 670 m. Relative proportions of fatty acids are derived from GC-FID peak areas and indicate that the total mesopelagic FA pool has a mass-weighted $\Delta^{14}C$ value of 68 ± 34‰ (Table S1). Assuming that biomass sinking from the surface is the only external contributor to this pool, it would carry the $\Delta^{14}C$ value of surface dissolved inorganic carbon (71 ± 3‰) (1). Some of our surface $\Delta^{14}C$ values from FA are lower than 71‰; however, the error ranges are large, and choosing a more positive end member yields the most conservative outcome (i.e., more in situ contribution). Creating an isotope mass balance between sinking material and the total sample, as was done in the main text, shows the maximum allowed (**I**) is 36% based on data in Table S2:

$$\Delta^{14}C_{\text{Mesopelagic\_FA\_min}} = (0.36)\left(\Delta^{14}C_{\text{Mesopelagic\_Bacteria\_max}}\right) + (0.64)\left(\Delta^{14}C_{\text{Sutface\_Biomass\_max}}\right)$$
$$\text{Solving: } (68 - 34‰) = 34‰ = (0.36)(-37‰) + (0.64)(71 + 3‰).$$

If the in situ component contributes 0–36% of total fatty acids collected at the mesopelagic depth, sinking material contributes 64–100%. The lower bound of this range is defined as line C in Fig. S5 (equivalent to the boundary of the solid solution field in Fig. 3 of the main text). Notably, this sinking component could derive from both bacterial and eukaryotic surface biomass, so it is not inconsistent with the estimate for sinking bacterial contribution calculated above. The boundary regions defined by lines A, B, and C in Fig. S5 suggest that if the sinking fraction **M** is defined by line C, it must consist mostly of material from the small particle size class.

The ^{14}C signature for $C_{18:1}$ fatty acid remains problematic. As stated above, isomers of $C_{18:1}$ are likeliest to have a large contribution from the in situ community, and yet their $\Delta^{14}C$ values are modern. It therefore seems that the total in situ mesopelagic $\Delta^{14}C$ value calculated above from DNA measurements could be too negative; either the cell count estimates underrepresent Archaea (10) or the absolute values reported for $\Delta^{14}C_{DNA}$ are too low (12). Either a greater contribution from modern DNA or greater numbers of Archaea are needed to reconcile all forms of data. Alternately, our mass-weighted total mesopelagic fatty acid $\Delta^{14}C$ value could be too positive. Minor compounds that could

not be resolved for ^{14}C measurement, particularly those commonly attributed to bacteria (e.g., branched and odd-chain fatty acids), potentially could represent the more ^{14}C-depleted component of the in situ bacterial community but are not counted here. Finally, it also is possible that there is a unique source of $C_{18:1\omega9}$ contributed by midwater zooplankton that consume sinking POM. In this way zooplankton potentially could edit the lipid composition of modern, sinking POM without contributing ^{14}C-modern DNA to the bulk DNA signature of the mesopelagic sample.

SI Text 7. Sequential Filtering Technique and Relation to Size Classes

We have simplified our interpretation of collected size classes by assigning a bacterial origin to the "picoplanktonic" fraction of fatty acids in calculation (*SI Text 5*) above, which results in a minimum **X** contribution outlined by dashed line D in Fig. S5. Koike et al. (13) found that, depending on filter type, 13–34% of bacterial cells in natural seawater passed through a 0.4- to 0.45-μm filter, so 66–87% would have been captured with the larger particulate size-class material. Similarly, we have found that *ca*. 50% of intact polar lipid (IPL)-membrane fatty acids associated with cells in the Eastern Tropical North Pacific pass through a glass microfiber grade GF/F (0.7-μm) filter and are captured on a 0.2-μm filter (14). Both findings suggest that size-based filtration achieves only partial separation of Bacteria. As noted in the main text, accounting for a significant portion of bacterial cells that we likely captured in the **L** (>0.5 μm) size class would reduce the calculated contribution from **X**. However, this means of estimating **X** both is a conservative minimum (because it derives from considering the full error range in calculations in ref. 1) and ultimately goes unused; the $^{14}C_{DNA}$ constraint from calculation (*SI Text 6*) above imposes a much more constrained minimum contribution from the **X** fraction (line C, Fig. S5).

Conversely, the use of cell counts in calculation (*SI Text 5*) also underestimates the contribution from the **X** size class: A significant fraction of submicron POM in the surface ocean likely exists in the form of detrital (nonliving, noncellular) particles (e.g., ref. 13). However, filtering can also break up fragile aggregates, and some of the detrital OM in the **X** fraction could have existed naturally in a larger size fraction. The estimate of a maximum 62% contribution from Bacteria likely is a low estimate for the maximum contribution from **X**, due to these additional detrital contributions. The striped solution field in Fig. S5 includes values for which total contribution from **X** is as great as 76%.

Finally, we believe that potential size-based biases due to adsorption of organic matter onto filters were avoided here by (*a*) directly extracting the filters rather than resuspending the POM from the solid surfaces and (*b*) avoiding use of glass fiber filters, which are known to adsorb dissolved organic matter (15). Our 0.5-μm filter was composed of cellulose ester and the 0.2-μm filter was polyethersulfone.

1. Ingalls AE, et al. (2006) Quantifying archaeal community autotrophy in the mesopelagic ocean using natural radiocarbon. *Proc Natl Acad Sci USA* 103(17):6442–6447.
2. Eglinton TI, Aluwihare LI, Bauer JE, Druffel ERM, McNichol AP (1996) Gas chromatographic isolation of individual compounds from complex matrices for radiocarbon dating. *Anal Chem* 68(5):904–912.
3. Pernthaler A, Pernthaler J, Amann R (2002) Fluorescence in situ hybridization and catalyzed reporter deposition for the identification of marine bacteria. *Appl Environ Microbiol* 68(6):3094–3101.
4. Teira E, Reinthaler T, Pernthaler A, Pernthaler J, Herndl GJ (2004) Combining catalyzed reporter deposition-fluorescence in situ hybridization and microautoradiography to detect substrate utilization by bacteria and Archaea in the deep ocean. *Appl Environ Microbiol* 70(7):4411–4414.
5. Shah SR, Pearson A (2007) Ultra-microscale (5-25 μg C) analysis of individual lipids by ^{14}C AMS: Assessment and correction for sample processing blanks. *Radiocarbon* 49(1): 69–82.
6. Lichtfouse E, Eglinton T (1995) ^{13}C and ^{14}C evidence of pollution of a soil by fossil fuel and reconstruction of the composition of the pollutant. *Org Geochem* 23:969–973.
7. Pearson A, Eglinton TI (2000) Sources of n-alkanes in Santa Monica Basin surface sediments: A model based on compound-specific ^{14}C and ^{13}C analysis. *Org Geochem* 30:1103–1116.
8. DeNiro M, Epstein S (1978) Influence of diet on the distribution of carbon isotopes in animals. *Geochim Cosmochim Acta* 42:495–506.
9. Blair N, et al. (1985) Carbon isotopic fractionation in heterotrophic microbial metabolism. *Appl Environ Microbiol* 50(4):996–1001.
10. Karner MB, DeLong EF, Karl DM (2001) Archaeal dominance in the mesopelagic zone of the Pacific Ocean. *Nature* 409(6819):507–510.
11. DeLong EF, et al. (2006) Community genomics among stratified microbial assemblages in the ocean's interior. *Science* 311(5760):496–503.
12. Hansman RL, et al. (2009) The radiocarbon signature of microorganisms in the mesopelagic ocean. *Proc Natl Acad Sci USA* 106(16):6513–6518.
13. Koike I, Shigemitsu H, Kazuki T, Kazuhiro K (1990) Role of sub-micrometre particles in the ocean. *Nature* 345:242–244.
14. Close H (2012) Size related isotopic heterogeneity in lipids from the marine water column. PhD thesis (Harvard Univ, Cambridge, MA).
15. Moran XAG, Gasol JM, Arin L, Estrada M (1999) A comparison between glass fiber and membrane filters for the estimation of phytoplankton POC and DOC production. *Mar Ecol Prog Ser* 187:31–41.
16. Brodie EL, et al. (2006) Application of a high-density oligonucleotide microarray approach to study bacterial population dynamics during uranium reduction and reoxidation. *Appl Environ Microbiol* 72(9):6288–6298.
17. DeSantis TZ, et al. (2007) High-density universal 16S rRNA microarray analysis reveals broader diversity than typical clone library when sampling the environment. *Microb Ecol* 53(3):371–383.

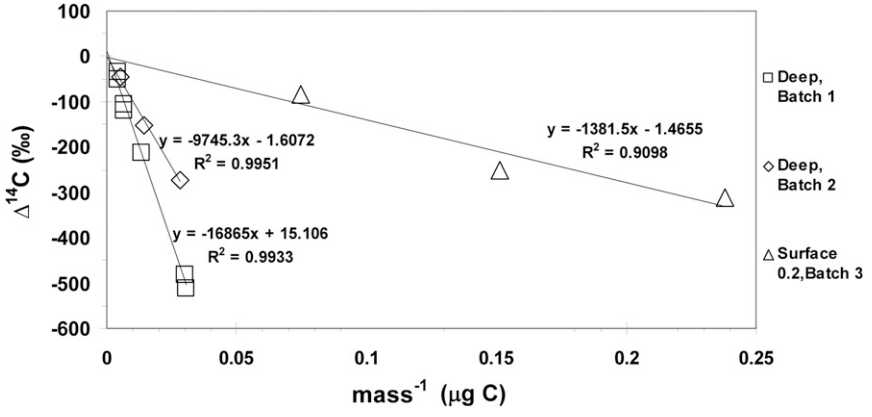

Fig. S1. Correlations between $\Delta^{14}C$ values and sample size for three sample sets, indicating a constant-mass addition of carbon from a contaminant to each sample in a given set. Projections of linear correlations were used to estimate the mass of the contaminant and, assuming a contaminant $\Delta^{14}C$ of −1,000‰, correct the sample $\Delta^{14}C$ values accordingly.

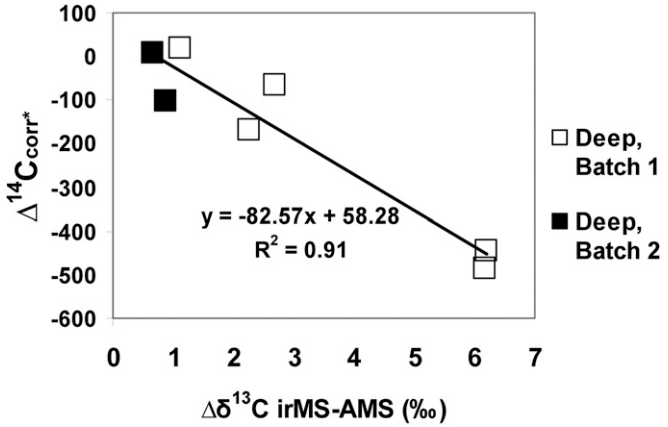

Fig. S2. Correlation between $\Delta^{14}C$ values (no residual correction) and the offset in $\delta^{13}C$ values derived from measurement by GC-C-irMS and AMS. Samples shown are only those for which AMS- and irMS-derived $\delta^{13}C$ values were available. All values have been corrected for addition of one carbon of known ^{13}C and ^{14}C content from methylation, and $\Delta^{14}C_{corr*}$ values also have been corrected for combustion blanks as described.

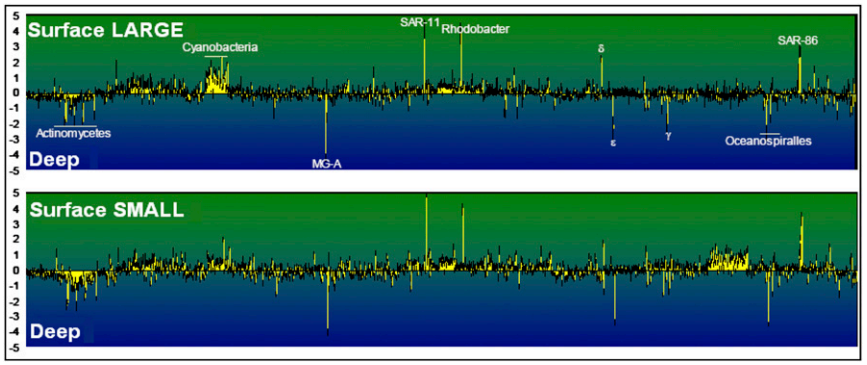

Fig. S3. Comparison of results for PhyloChip analysis of DNA. Plots are difference spectra, calculated for each OTU (*x* axis) on a logarithmic scale of hybridization intensity (*y* axis). The data show that similar communities of Bacteria were retained on both the surface (21 m) large size class (>0.5 μm) and the small size class (0.2–0.5 μm) filters; but when each is compared with the deep (670 m) filter, significant differences are detected across OTUs consistent with expected surface and pelagic populations. Yellow peaks represent differences that are significant beyond the error range of the hybridization signal; black peaks are within error ranges and thus insignificantly different for the abundance of the OTU.

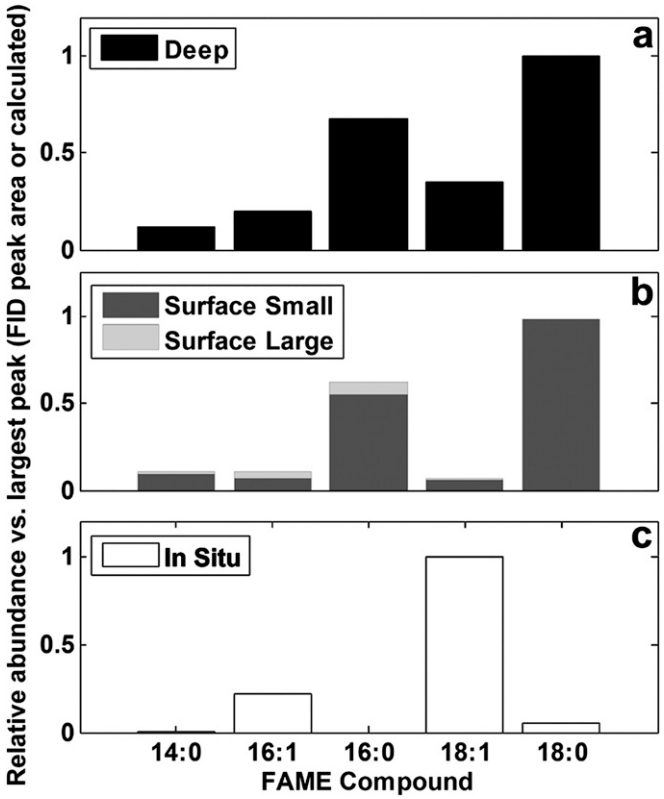

Fig. S4. (*A*) Fatty acid profile of actual mesopelagic total suspended organic matter (>0.2 μm), as fatty acid methyl esters (FAMEs) detected quantitatively by flame ionization detection (FID). (*B*) Modeled profile of hypothetical maximized sinking material **M** that is 88% surface small X-POM (0.2–0.5 μm) and 12% surface large (>0.5 μm). (*C*) Derived profile of hypothetical in situ fatty acids **I** for the case in which the surface sinking contribution to **D** is maximized. Profile **I** is calculated as the residual when the modeled profile **M** shown in *B* is subtracted from the observed profile **D** shown in *A*.

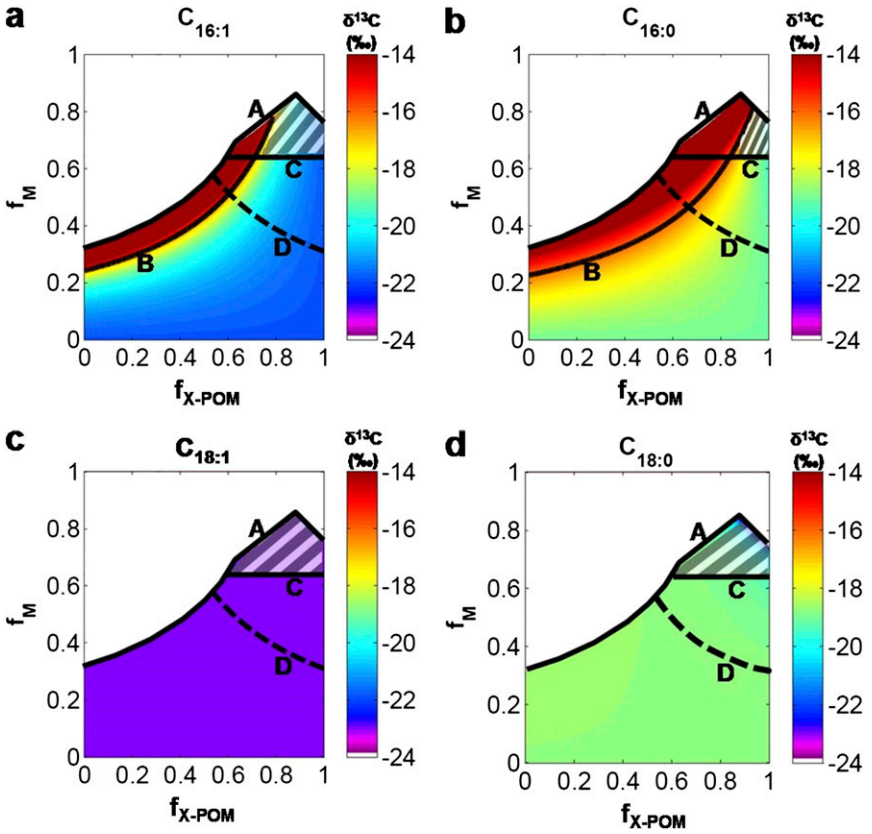

Fig. S5. Modeled $\delta^{13}C$ values of four individual fatty acids from the in situ mesopelagic bacterial community (*A*, $C_{16:1}$; *B*, $C_{16:0}$; *C*, $C_{18:1}$; *D*, $C_{18:0}$), calculated over all f_X (*x* axis, proportion sinking from **X**, where **X** + **L** = **M**) compositions contributing to **M** (total sinking) and all allowed f_M (*y* axis, total proportion sinking: **M** + **I** = **D**) contributing to **D** (see text for definition of allowed). The colored fields, delineated by line A, represent all solutions allowable based on mixing of fatty acid profiles (equivalent to the solution field with light shading in Fig. 3 of the main text). We stipulate that the upper limit for modeled $\delta^{13}C$ values in the in situ population is −16‰, implying that results above the contour marked "B" (*A* and *B*) are excluded. Solutions below line B are equivalent to the solution field with dark shading in Fig. 3 of the main text. Additional constraints on **X**:**L** ratios and **M**:**I** ratios imposed by ancillary data further constrain the estimated results to the striped areas (*A*–*D*). Dashed line D is defined as the lower bound on contribution to deep fatty acids from sinking surface bacterial biomass (operationally equated to the **X** size fraction; $f_X \times f_M \geq 31\%$). Line C is defined as the minimum fraction of the total deep sample **D** that must come from the sinking flux **M** ($f_M \geq 64\%$), based on ^{14}C content of mesopelagic DNA and lipids. Isotopic mass balance must be reached for all compounds simultaneously; the narrowest solution field (striped area in *B*) is thus the best constrained (equivalent to the solid solution field in Fig. 3 of the main text).

Table S1. Data for fatty acids

	Deep (>0.2 μm)										Surface 0.2–0.5 μm										Surface >0.5 μm									
FAME	Rel abun	$\delta^{13}C$	±σ	$\Delta^{14}C_{raw}$	±σ	$\Delta^{14}C_{corr}$	±σ	Notes	Size, μg C	AMS ID	Rel abun	$\delta^{13}C$	±σ	$\Delta^{14}C_{raw}$	±σ	$\Delta^{14}C_{corr}$	±σ	Notes	Size, μg C	AMS ID	Rel abun	$\delta^{13}C$	±σ	$\Delta^{14}C_{raw}$	±σ	$\Delta^{14}C_{corr}$	±σ	Notes	Size, μg C	AMS ID
14:0	0.18	−18.3	0.2	−467	14	114	76	*,†,‡	24	OS-49294	*0.17*	—	—	*−392*	*17*	*−201*	*261*	*,†,¶	7	Irvine	0.22	−25.3	0.2	—	—	—	—		—	—
i+a-15:0	—	—	—			—	—				—	—	—	—	—	—	—		—	—	0.13	−22.7	0.3	−33	8	48	14	*,†,‖	105	OS-66618
16:1	0.29	−21.7	0.2	−264	12	66	47	*,†,§	36	OS-67905	0.13	−22.4	0.2	—	—	—	—		—	—	0.51	−23.8	0.1	—	—	—	—		—	—
Repeat				*−295*	*4*	*399*	*77*	*,†,‡	*12*	*(Irvine)*																				
6:0	1.00	−18.8	0.2	−119	8	49	12	*,†,‡	103	OS-49279	1.00	−19.0	0.2	−76	9	86	28	*,†,¶	17	Irvine	1.00	−23.6	0.2	−14	4	51	5	*,†,‖	296	OS-65816
Split				−106	8	65	13	*,†,‡	34	CAMS 114840																				
17:1	0.15	−25.0	0.2			—	—				0.12	−22.8	0.7	—	—	—	—		—	—	—	—	—	—	—	—	—		—	—
17:0	0.09	−21.5	0.2	−496	13	57	74	*,†,‡	23	OS-49295	0.07	—	—	−246	13	86	112	*,†,¶	7	Irvine	0.03	—	—	—	—	—	—		—	—
18:1	0.52	−22.7	0.2	−208	11	72	25	*,†,‡	50	OS-49286	0.11	−23.3	0.3	−226	13	−2	58	*,†,¶	9	Irvine	0.14	−23.5	0.8	−13	7	52	10	*,†,‖	163	OS-66611
Repeat				−148	13	43	24	*,†,§	70	OS-66625												−22.0	1.2							
18:0	1.48	−18.5	0.2	−35	8	99	10	*,†,‡	153	OS-49272	1.78	−18.8	0.2	—	—	—	—		—	—	0.05	−23.7	1.5	7	12	93	23	*,†,‖	60	OS-67899
Split				−49	7	82	9	*,†,‡	58	CAMS 114841																				
Repeat				−45	9	60	11	*,†,§	138	OS-66614																				
20:5	—	—	—	—	—	—	—			—	—	—	—	—	—	—	—		—	—	0.27	−25.7	0.9	—	—	—	—		—	—
22:0	—	—	—	—	—	—	—			—	—	—	—	—	—	—	—		—	—	*0.03*	—	—	*−278*	*14*	*−225*	*24*	*,†,‖	*46*	*OS-67906*
19:0 standard	—	—	—	—	—	—	—			—	—	—	—	—	—	—	—		—	—	0.07	−31.7	0.1	−4	11	71	19	*,†,‖	78	OS-66626
19:0 standard orig.	—	−31.7	0.1	71	4	71	4	*	242	OS-67848																				

Relative abundance, $\delta^{13}C$, $\Delta^{14}C$ (raw and corrected), and AMS measurement information are shown. Isomers of monounsaturated acids were combined for isotope analysis. Samples in italics were eliminated due to small size and/or unidentified contamination. Corrections were applied. Compounds with no reported values had insufficient quantity for measurement. Rel abun, relative abundance.

*Combustion blank (1.0 μg C).

†Methyl carbon.

‡Residual correction, batch 1 (16.6 μg C).

§Residual correction, batch 2 (9.8 μg C).

¶Residual correction, batch 3 (1.4 μg C).

‖Internal standard correction, batch 4 (1.7 μg C).

Table S2. Ancillary data used for model calculations

	Mean	± σ	Reference
Surface DIC $\Delta^{14}C$	71	3	I
Deep DIC $\Delta^{14}C$	−151	3	I
Surface DNA			
0.2–0.5 μm $\Delta^{14}C$	60	3	H
670 m DNA			
0.2–0.5 μm $\Delta^{14}C$	−140	17	H
>0.5 μm $\Delta^{14}C$	−73	4	H
670-m Archaeal lipid			
Average in situ $\Delta^{14}C$, calculated	−112	28	I
Fraction from sinking	0.14	0.07	I
Fatty acids: 16:1, 16:0, 18:1, 18:0			
20-m FA, small			
Mass-weighted $\Delta^{14}C$	78	66	C
20-m FA, large			
Mass-weighted $\Delta^{14}C$	52	13	C
670-m FA			
Mass-weighted $\Delta^{14}C$	68	34	C
25-m cell counts			
Archaea cells/mL	3.78*E*+04	3.88*E*+04	K-supp
Bacteria cells/mL	3.07*E*+05	1.03*E*+05	K-supp
Archaea + Bacteria cells/mL	3.45*E*+05		
Fraction Bacterial	0.89	0.11	
500-m cell counts			
Archaea cells/mL	2.26*E*+04	9.04*E*+03	K-supp
Bacteria cells/mL	3.01*E*+04	1.03*E*+04	K-supp
Archaea + Bacteria cells/mL	5.27*E*+04		
Fraction Bacterial	0.57	0.12	

H, Hansman et al. (12); I, Ingalls et al. (1); C, Close et al. (this paper); K-supp, Karner et al. (10), supporting information.